Study of the mass transfer phenomena involved in an electrophoretic membrane contactor

Sylvain Galier, Hélène Roux-de Balmann

Study of the mass transfer phenomena involved in an electrophoretic membrane contactor

Sylvain Galier, Hélène Roux-de Balmann*

Laboratoire de Génie Chimique, CNRS UMR 5503, Université Paul Sabatier, 118 Route de Narbonne, 31062 Toulouse Cedex 4, France

Abstract

Electrophoretic separators, in which a porous membrane is used as a contactor, offer the possibility to scale up electrophoresis as well as to extend the field of application of electrodialysis to fractionate polyamino acids, peptides or small proteins for instance. This paper deals with the study of the mass transfer mechanisms involved in such electroseparation processes. On one hand, a theoretical approach is carried out. The different contributions to the mass transfer are considered in order to establish a relationship providing the solute concentration as function of the main parameters of the system, i.e. the operating conditions and the membrane, buffer and solute characteristics. In this expression, a partition coefficient is used to represent the interactions taking place at the membrane–solution interface. Then, an experimental study is performed with different representative solutes using a prototype apparatus in order to determine the dependence of the solvent and solute transfer with respect to the operating and physicochemical parameters of the system. The experimental results show the existence of a limiting electro-osmotic flux, the origin of which is explained. Then the partition coefficient is determined for any set of conditions by fitting the variations of the solute concentration calculated by the model with experimental ones. The dependence of the partition coefficient with respect to the solute and buffer characteristics, together with that of the transmission coefficient obtained during filtration experiments, shows that the main limitation with respect to the mass transfer is due to electrostatic interactions taking place at the membrane–solution interface.

Keywords: Membrane; Separation process; Electrophoresis; Electro-osmosis; Mass transfer

1. Introduction

Because of the expansion of biotechnology, there is an increasing demand concerning processes capable of producing molecules at a very high level of purity, while fully preserving their biological functions or properties of use.

A wide range of separation processes can be operated to separate, concentrate or purify biological molecules. They are commonly classified within three groups, clarification, extraction and purification, according to their productivity and selectivity.

Electrophoresis is an electrically driven operation, that constitutes a purification step used to remove rem- aining impurities the properties of which are very close to those of the target molecule. As far as analysis of biological molecules is concerned, electrophoresis, mainly carried out in supported media

* +
+

Nomenclature

C	solute concentration ($kg\,m^{-3}$, i.e. $g\,l^{-1}$)
$\bar{C}$	solute concentration in the membrane ($kg\,m^{-3}$, i.e. $g\,l^{-1}$)
C_0	inlet solute concentration ($kg\,m^{-3}$, i.e. $g\,l^{-1}$)
C_i	ionised species concentration ($mol\,l^{-1}$)
d	concentrate and dilute compartment thickness (m)
E	electric field in the bulk solution ($V\,m^{-1}$)
$\bar{E}$	electric field in the membrane ($V\,m^{-1}$)
h	cell height (m)
i	current (A)
I	ionic strength ($mol\,l^{-1}$)
J_{eo}	electro-osmotic flux ($m\,s^{-1}$)
l	cell length (m)
N	solute flux in the solution ($kg\,m^{-2}\,s^{-1}$)
$\bar{N}$	solute flux through the membrane ($kg\,m^{-2}\,s^{-1}$)
pK	acidic constant dissociation
Q	flow rate ($m^3\,s^{-1}$ or $ml{\cdot}h^{-1}$)
S	membrane area (m^2)
T	transmission coefficient
u_{eo}	electro-osmotic mobility ($m^2\,V^{-1}\,s^{-1}$)
u_{mi}	electrophoretic mobility ($m^2\,V^{-1}\,s^{-1}$)
z	co-ordinate (m)
z_i	valence

Greek letters

α	slope of the straight line $u_{eo} = f(E\tau)$
α_0	y-intercept of the straight line $u_{eo} = f(E\tau)$
χ	electrical conductivity ($S\,m^{-1}$)
ε	membrane porosity
ε_0	dielectric constant of vacuum ($C^2\,J^{-1}\,m^{-1}$)
ε_r	relative dielectric constant of water
ϕ	partition coefficient
μ	dynamic viscosity (Pa s)
τ	mean residence time (s)
ζ	membrane zeta potential (V)

Subscripts

avg	average
c	concentrate
d	dilute
eo	electro-osmosis
f	feed
mi	electromigration
p	permeate
s	solute

like thin gels for instance, is recognised as a very efficient technique because of its high resolution [1]. Consequently, different ways were investigated to use electrophoresis at the so-called "preparative scale", i.e. for production purpose.

Direct extrapolation of analytical techniques was first considered by increasing the size, i.e. the thickness, of the gels used for analysis, or the amount of product deposited in these gels. However, very poor resolution was obtained compared to that observed at the analytical scale. Other quite different modes of operation, were thus, considered in which electrophoresis is carried out in a flowing buffer film [2–4]. In this manner, continuous separation as well as direct recovery of the purified fractions, i.e. avoiding any further elution step, are obtained. The principle of continuous flow electrophoresis (CFE), which is the most common of these, has been described previously [5,6]. Different experimental and theoretical studies were carried out so as to understand the different transport phenomena involved in the process. The performances of CFE have also been extensively studied with synthetic solutions as well as with real biological samples [7–9]. From these works, the limitations of CFE were pointed out and their origin was also identified. It was demonstrated that the main limitation is due to buoyancy-driven convection (Joule heating and mass transfer) [10,11]. Consequently, the operating conditions are restricted to those capable of maintaining a stable buffer and sample flows in the electrophoresis chamber. Correlations involving adimensional numbers were proposed to find operational domains in which proper separation can be achieved [9]. The tight relationship between productivity and resolution, i.e. purity, was also demonstrated. Finally, it was found that the productivity cannot be increased over a certain limit, typically about few milligrams per hour.

In order to overcome these limitations, other apparatus were developed, in which the separation is carried out in a multicompartment separation chamber. The different compartments are delimited by membranes

acting as screeners or contactors [12–14], so as to avoid the mixing of solutions. These electromembrane operations have two common characteristics. Firstly, the selectivity comes from the different solute flow rates through the membrane. Then, the productivity can be increased by increasing the number of separation chambers without significantly damaging the selectivity.

The most common electromembrane operation is electrodialysis (ED), in which ion exchange membranes are used. The main applications of electrodialysis concern the concentration or demineralisation of solutions containing ionic species. To some extent, ED can also be operated for purification, since the separation of neutral, like sugars, from ionic species can be achieved [15]. However, because of the properties of the membranes, the migration of molecules of molecular weight exceeding about 500 Da is forbidden.

The use of porous membranes in replacement of ion exchange ones was then investigated so as to extend the field of application of electrodialysis to biological molecules like polyamino acids, peptides or proteins. In that case, the porous membrane acts as a contactor and the separation is achieved with respect to the difference between the mass flow rates of the species. According to the membrane and solute properties, this difference can have various origins, like different electrophoretic mobility, sieving effects or a coupling of both. Then, different arrangements and different types of membranes can be used to achieve different kind of purification. Previous experimental works were carried out during which the separation of proteins, like haemoglobin and serum albumin [14], or the recovery of enzymes, like lipase [16], was investigated. From these studies, the influence of the porous membrane on the mass transfer was pointed out [14]. However, on the contrary to other electrically driven separations, like free flow electrophoresis or electrodialysis for instance, no comprehensive work was devoted to the understanding of the transfer phenomena, the coupling of which determines the performances of the separation.

In this context, the aim of the present paper is to study the mass transfer involved in electroseparation processes using porous membranes as contactors. This study is carried out by associating a theoretical approach with an experimental work. A model is proposed in which the different contributions to the mass transfer are considered to get expressions of the outlet concentrations with respect to the operating conditions and to the membrane and solutes relevant characteristics.

Then, an experimental work is performed with a dedicated separation chamber and different solutes so as to investigate the influence of the solute charge and size as well as that of the main operating parameters. Calculated and experimental results are compared in order to determine the mass transfer limitations.

2. Theoretical approach

A theoretical approach is carried out in order to develop a mathematical model to calculate the concentrations at the outlet of the separation chamber as function of the operating parameters and solute characteristics. The principle of the process under study is first presented. Then, the different transport phenomena that take place in the separation chamber, i.e. in the solution and at the membrane–solution interface, are discussed. Finally, a model is established by considering the coupling of these contributions and their influence on the solvent and solute mass transfer.

2.1. Description of the process

The principle of the electroseparation process under study is illustrated in Fig. 1. The separation chamber

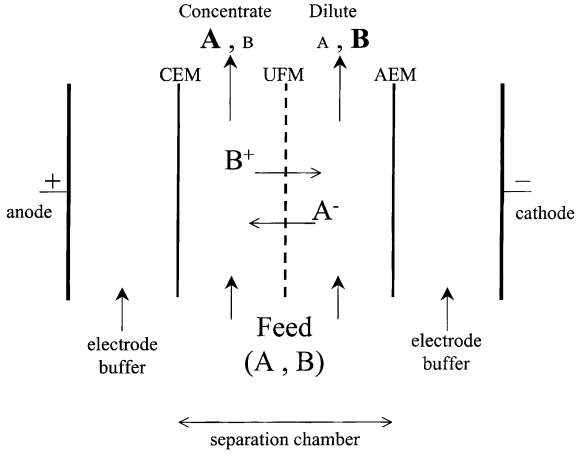

Fig. 1. Schematic drawing of the electrophoretic membrane contactor. UFM: ultra-filtration membrane; AEM: anion exchange membrane; CEM: cation exchange membrane.

itself is composed of two adjacent compartments delimited by a porous membrane, like an ultra-filtration one for instance. This membrane acts as a contactor between the two streams between which the mass transfer takes place. The buffered solution to be purified is continuously fed on both sides of the membrane. The only driven force is a voltage, applied in a direction perpendicular to the feed flow. Two electrodes are located in dedicated compartments, which are isolated from the separation chamber itself by ion exchange membranes. As soon as a voltage is applied, the charged components contained in the feed migrate along the chamber thickness from one compartment toward the other through the porous membrane. The solute mass flow depends on its electrophoretic mobility, which is fixed by the pH of the buffered solution. Then, solutes having distinct electrophoretic mobilities are carried through the membrane at different rates. Two outlet streams with different compositions, are thus, obtained. The compartments in which the outlet concentration of the target solute are respectively, lower and higher than the inlet one will be further called "dilute" and "concentrate".

2.2. Transport phenomena

The application of an electric field gives rise to two phenomena: electromigration of charged solutes and electro-osmosis through the charged porous membrane.

For a given solute, the mass flux density due to electromigration, N_{mi}, is given by the following relationship:

$$N_{\mathrm{mi}} = u_{\mathrm{mi}} E C \tag{1}$$

where E is the electric field, C the solute concentration and u_{mi} its electrophoretic mobility. This electrophoretic mobility is a solute characteristic that depends on the pH, ionic strength and temperature of the solution. As former explained, electromigration is the separative effect of the process under study. However, as far as a voltage is applied, other induced phenomena take place and combine with electromigration to govern the mass transfer that fixes the separation performances.

The most significant one is electro-osmosis due to the electrical charges carried by the membrane surface. When the membrane is put into contact with an electrolyte solution, a double layer takes place in which these surface charges are compensated by ones of opposite sign present in the electrolyte. Under the influence of the electric field, the ions in this double layer migrate toward the electrode of opposite sign, carrying solvent. The resulting solvent flow is the electro-osmotic flux [17]. The electro-osmotic flux density (J_{eo}) is proportional to the electric field E. The constant of proportionality defines the electro-osmotic mobility u_{eo}

$$J_{\mathrm{eo}} = u_{\mathrm{eo}} E \tag{2}$$

This electro-osmotic mobility depends on the membrane characteristics, like the electrical charge and the pore size, as well as on those of the electrolyte, like the pH, the ionic strength or the ionic composition.

The solute flux density resulting from electro-osmosis, N_{eo}, is given by the following equation

$$N_{\mathrm{eo}} = J_{\mathrm{eo}} C = u_{\mathrm{eo}} E C \tag{3}$$

As far as the double layer thickness is small compared to the membrane pore size, the following explicit Helmoltz–Smoluchowski relationship can be used between the electro-osmotic flux and the membrane zeta potential

$$J_{\mathrm{eo}} = \frac{i \varepsilon_0 \varepsilon_{\mathrm{r}} \zeta}{\mu \chi S} \tag{4}$$

This relationship is commonly used to calculate membrane zeta potential from experimental variations of the electro-osmotic flux versus the current density [18,19].

2.3. Mathematical model

It is considered that the solute flux due to electromigration, directed from the dilute toward the concentrate, is positive. In the present study, the ultrafiltration membrane used carries negative charges, so that electro-osmosis is directed toward the cathode. On the other hand, for the pH values investigated, the solutes are negatively charged. Then, electro-osmosis and electromigration are oriented in opposite directions and the electro-osmotic flux will be negative.

The solute mass balance is written at steady-state by considering the mass transfer phenomena described

previously, i.e. the convection due to electro-osmosis and electromigration. The Nernst–Plank equation is established at a given position z along the chamber height, in the solution and in the membrane.

During the experiments, the outlet flow rates in the dilute and the concentrate are set to constant and identical values ($Q_c = Q_d = Q$). Then, because of the electro-osmotic flux through the membrane, the flow rate in each compartment varies along the chamber height.

The steady-state conservation equation is written in each compartment for a thin element of the separation chamber taken in the flow axis z.

$$Q_c(z) - Q_c(z+dz) - J_{eo} l\, dz = 0 \quad \text{with } J_{eo} > 0 \tag{5}$$

$$Q_d(z) - Q_d(z+dz) + J_{eo} l\, dz = 0 \tag{6}$$

Assuming that the electro-osmotic flux density, J_{eo}, remains constant, former equations can be integrated to get

$$Q_c(z) = Q_c + J_{eo} l (h - z) \tag{7}$$

$$Q_d(z) = Q_d - J_{eo} l (h - z) \tag{8}$$

where Q_c and Q_d are the outlet flow rates.

Then, assuming that the total flow rate remains constant, the inlet flow rates are provided by the following relationships:

$$Q_c^{inlet} = Q_c + J_{eo} S \tag{9}$$

$$Q_d^{inlet} = Q_d - J_{eo} S \tag{10}$$

where S is the total membrane surface.

On the other hand, as far as the solute mass balance is expressed, following equations are obtained:

$$Q_c(z) C_c(z) - Q_c(z+dz) C_c(z+dz) + N_s(z) l\, dz = 0 \tag{11}$$

$$Q_d(z) C_d(z) - Q_d(z+dz) C_d(z+dz) - N_s(z) l\, dz = 0 \tag{12}$$

It is considered that the solute transfer results from the coupling of the convection due to electro-osmosis with electromigration. It means that the contribution of osmosis and diffusion to the solvent and solute transfer is neglected. This assumption will be later validated experimentally. The variation of the concentration along the compartment thickness is neglected compared to that along the z-axis. It is further assumed that the electrophoretic and electro-osmotic mobilities as well as the solute concentration remain constant across the membrane. Then, at steady-state the solute flux through the membrane can be written as

$$\begin{aligned} \bar{N}_s(z) &= u_{mi} \bar{E} \bar{C}(z) - u_{eo} \bar{E} \bar{C}(z) \\ &= (u_{mi} - u_{eo}) \bar{E} \bar{C}(z) \end{aligned} \tag{13}$$

where $\bar{E}$ is the electric field in the membrane. u_{mi} and u_{eo} are the absolute values of the electrophoretic and electro-osmotic mobilities.

Assuming that the current is mainly carried by the electrolyte ions and that the electrical conductivity within the membrane pores is the same as that in the solution, the electric field in the membrane, $\bar{E}$, is linked to that in the bulk solution, E, by the following expression [20]:

$$\bar{E} = \frac{E}{\varepsilon} \tag{14}$$

where ε is the membrane porosity.

Then, the following relationship is used to link the concentrations in the solution and in the membrane:

$$\bar{C}(z) = \phi C_d(z) \tag{15}$$

where ϕ is a partition coefficient, the value of which is comprised between 0 and 1.

This kind of approach involving a partition coefficient, ϕ, was first proposed by Ferry [21] to express a partition due to steric effects taking place at the membrane–solution interface. It was then extended to consider other kinds of contributions, like electrostatic interactions for instance [22,23]. Theoretical expressions of the partition coefficient were proposed involving the potential energy of interaction between the solute and the membrane. But, since this value is quite hardly accessible, direct calculation of the partition coefficient remains still problematic. Then, this partition coefficient is mainly used as a fitted value, which has to be determined from experimental results. From the qualitative point of view, whatever the origin of these interactions, the value of ϕ is quite helpful to evaluate the strength of the membrane–solute interactions. More precisely, decreasing values of ϕ reveal stronger interactions.

The solute flux through the membrane can be obtained by combining Eqs. (13) and (15):

$$\bar{N}_s(z) = \frac{\phi}{\varepsilon}(u_{mi} - u_{eo})EC_d(z) \tag{16}$$

On the other hand, the continuity equation at steady-state allows to link the solute flux through the membrane to the solute flux in the dilute by the relation

$$\bar{N}_s(s) = \frac{N_s}{\varepsilon} \tag{17}$$

Combining Eqs. (16) and (17), one gets:

$$N_s(z) = \phi(u_{mi} - u_{eo})EC_d(z) \tag{18}$$

This expression of the solute flux is substituted in Eq. (12). Then, the resulting equation is integrated and the following expression is obtained:

$$C_d(z) = C_0\left[\frac{Q_d - J_{eo}S}{Q_d - J_{eo}l(h-z)}\right]^{[(\phi(u_{mi}/u_{eo})-1)+1]} \tag{19}$$

Finally, the expression of the outlet concentration, i.e. at $z = h$, is given by

$$C_d = C_0\left[1 - \frac{J_{eo}S}{Q_d}\right]^{[(\phi(u_{mi}/u_{eo})-1)+1]} \tag{20}$$

The mean residence time, τ, in the chamber is defined as the ratio of the compartment volume over the flow rate, i.e.

$$\tau = \frac{V}{Q_d} = \frac{dS}{Q_d} = \frac{dlh}{Q_d} \tag{21}$$

Then, combining Eqs. (20) and (21), one gets

$$C_d = C_0\left[1 - \frac{u_{eo}E\tau}{d}\right]^{[(\phi(u_{mi}/u_{eo})-1)+1]} \tag{22}$$

where d is the compartment thickness.

Finally, the outlet concentration in the concentrate C_c is obtained from the solute mass balance. As far as the inlet concentrations are identical and equal to C_0, this mass balance is

$$C_c = 2C_0 - C_d \tag{23}$$

2.4. Discussion

The validity domain of Eq. (22) is determined with respect to the following considerations. Because the inlet flow rates in both compartments, dilute and concentrate, are superior to zero, the operating conditions are restricted to those for which the electro-osmotic flow, equal to $J_{eo}S$, is lower than the outlet flow rates, Q_c and Q_d. As already explained, these flow rates are fixed and equal so that $Q_c = Q_d = Q$. On the other hand, the electro-osmotic flow is directed from the concentrate to the dilute. Then, former condition is expressed by the following relationship:

$$0 < \frac{J_{eo}S}{Q} < 1 \quad \text{or} \quad 0 < \frac{u_{eo}E\tau}{d} < 1 \tag{24}$$

As far as the electro-osmotic tends towards zero, the outlet concentration in the dilute, provided by Eq. (22) becomes:

$$C_d = C_0 \exp\left[-\frac{\phi u_{mi}E\tau}{d}\right] \tag{25}$$

This equation is similar to that established in previous work [14] in which an apparent electrophoretic mobility was defined. This mobility is in fact the product of the partition coefficient by the true electrophoretic mobility, i.e. ϕu_{mi}.

Finally, Eq. (22) shows that the outlet concentrations depend on several parameters which have different origins. The half-thickness of the separation chamber, d, is the only parameter tight to the chamber geometry. The electrophoretic mobility depends on the solute itself as well as on the pH of the separation buffer. The partition coefficient and the electro-osmotic mobility depend on the membrane and solute charges and sizes. So, these two parameters depend on the pH and ionic strength of the solution. It was also demonstrated that the charge of the membrane can change according to that of the solute [24,25]. Finally, the influence of the operating conditions is described through the value of $E\tau$, which is the product of the electric field by the residence time. This parameter was also pointed out as a characteristic parameter during previous works devoted to the study of the transport phenomena involved in free flow electrophoresis [9].

3. Materials and methods

3.1. Buffer and samples

All chemicals used are of analytical grade. Poly(L-glutamic) acid (PLGA), α-lactalbumin (type III from bovine milk), polyethylenglycol (PEG) and 2-(*N*-morpholino)ethane-sulfonic acid (MES) were purchased from Sigma (St. Louis, MO, USA). Tris(hydroxymethyl)aminomethane (Tris) was a product from Merck (Darmstadt, Germany).

The fluid used as separation buffer as well as electrode buffer is a Tris–Mes buffer at pH of 8.0. The electrical conductivities are 140 $\mu S\,cm^{-1}$ for the separation buffer and 220 $\mu S\,cm^{-1}$ for the electrode buffer. The solutions are prepared by dissolving the appropriate amount of poly(L-glutamic) acid, α-lactalbumin or PEG in the separation buffer.

3.2. Electroseparation apparatus and set-up

The general design of the electrophoretic chamber was depicted in Fig. 1. The prototype cell used in this work is 16 cm long and 2 cm wide, so that the membrane active area is 32 cm^2. The thickness of the electrode, dilute and concentrate compartments is 1.0, 0.2 and 0.2 cm, respectively. The porous membrane is a derived cellulose membrane made in our laboratory. Its hydraulic permeability is equal to 4.0×10^{-10} m $Pa^{-1}\,s^{-1}$ and its molecular weight cut-off is estimated about 100 kD. A cation exchange membrane and an anion exchange membrane are used at the anode and cathode side, respectively. These membranes are Neosepta CMX and AMX (Tokuyama corporation, Japan).

Plastic mesh screens are inserted between each membrane pair so as to control the compartment thickness and to act as turbulence promoters. Two platinum grids with an area of 36 cm^2 are used as electrodes.

The experimental set-up is depicted in Fig. 2. The two separation compartments are continuously fed from two distinct feed tanks using peristaltic pumps placed at the outlet of the cell. The outlet flow rates are set at constant and equal values. The electrode buffer is circulated in a closed loop from a single tank to the electrode compartments using a gear pump.

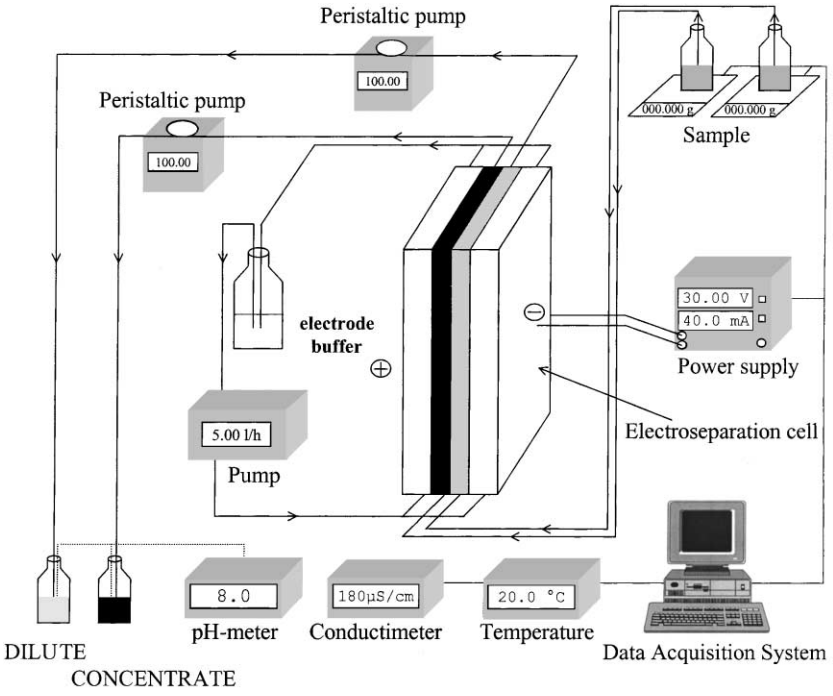

Fig. 2. Description of the experimental set-up.

An automatic data acquisition system allows real-time recording of the main experimental data, i.e. inlet flow rates, inlet and outlet conductivities and pH, current, voltage and temperatures.

3.3. Experimental procedure and operating conditions

All experiments are carried out at the ambient temperature ($22 \pm 3^{\circ}$C).

Buffered solutions are used with single solute, the inlet concentration of which is set at a constant value of $0.1\,\mathrm{g\,l^{-1}}$.

Different outlet flow rates in the separation chamber are used ranging from 75 to $150\,\mathrm{ml\,h^{-1}}$. The buffer flow rate in the electrode compartment is fixed at $5.01\,\mathrm{h^{-1}}$.

The experiments are carried out at a constant current density. Different values are used ranging from 10 to 70 mA (i.e. from 3 to $22\,\mathrm{A\,m^{-2}}$).

The average electric field strength, E in the separation chamber is calculated from the following equation [20]:

$$E = \frac{i}{\chi_{\mathrm{avg}} S} \tag{26}$$

where i is the current, S the membrane area and χ_{avg} the mean electrical conductivity calculated from the measurement of the inlet and outlet conductivities. For the operating conditions used, the average electric field is comprised between 100 and $900\,\mathrm{V\,m^{-1}}$.

Since the outlet flow rates are fixed and equal, the electro-osmotic flux density, J_{eo} is obtained from the measurement of the inlet flow rates in each compartment by the following relationship:

$$J_{\mathrm{eo}} = \frac{|Q_{\mathrm{c}}^{\mathrm{inlet}} - Q_{\mathrm{d}}^{\mathrm{inlet}}|}{2S} \tag{27}$$

Then the electro-osmotic mobility is calculated from Eq. (2), in which the electric field is provided by former Eq. (26).

The solute concentration is determined every 5 min in both compartments. The analytical methods are described hereafter.

Finally, the evaluation of the contribution of osmosis and diffusion is carried out. In that case, one compartment is fed with a buffered solution of PLGA or α-lactalbumin at $0.1\,\mathrm{g\,l^{-1}}$, while the other is fed with the buffer. The flow rate is set at the lowest value, i.e. $75\,\mathrm{ml\,h^{-1}}$. The variation of the inlet flow rates and of the solute concentrations are followed versus time, without applying any voltage.

3.4. Data acquisition

The different methods used to determine the parameters involved in the expression of the concentration established in Section 2 are described hereafter.

3.4.1. Concentration measurements

Poly(L-glutamic) acid concentrations are determined by gel permeation chromatography with UV detection at 214 nm, using a Superdex peptide column (Pharmacia Biotech, Sweden). The eluent is a phosphate buffer at pH 7.2 adjusted with NaCl to get a conductivity of $10\,\mathrm{mS\,cm^{-1}}$, at a flow rate of $0.80\,\mathrm{ml\,min^{-1}}$. The concentration of α-lactalbumin is measured by ultraviolet spectroscopy at 280 nm. PEG concentrations are determined by gel permeation chromatography with refractive index detection, using a TSK G2000PW column. The eluent is desionised water at a flow rate of $1.00\,\mathrm{ml\,min^{-1}}$.

3.4.2. Electrophoretic mobility

The electrophoretic mobilities of poly(L-glutamic) acid and α-lactalbumin are determined in the separation buffer at pH of 8.0 by capillary electrophoresis with a Spectra Phoresis 500 (Spectra-Physics, United States).

3.4.3. Ionic strength calculation

The relevance of the knowledge of the ionic strength will be discussed in Section 4. A correlation was searched to calculate this ionic strength from the experimental measurement of the electrical conductivity without requiring the knowledge of the ionic composition of the solution. Indeed, this composition, quite hardly accessible, varies during the experiments because of the migration of the buffer ions through the membranes.

On one hand, buffer solutions at pH 8 containing different known concentrations of Tris and Mes were prepared. The corresponding electrical conductivity was measured.

On the other hand, the ionic strength, I was calculated from the ionised species concentrations (C_i) and their valence (z_i):

$$I = \sum_i z_i^2 C_i \tag{28}$$

The concentrations of H^+ and OH^- are calculated from the pH and the water equilibrium constant. Then, the concentrations of ionic species ($[A^-]$ and $[BH^+]$) are calculated from the following equilibrium:

$$\text{weak acid}: \quad AH \Leftrightarrow H^+ + A^- \quad (pK_1)$$
$$\text{weak base}: \quad BH \Leftrightarrow H^+ + B \quad (pK_2)$$

and the total acid or base concentrations (C_A and C_B). The values of pK_1 and pK_2 at 20°C are equal to 6.05 and 7.92, respectively [26].

Then, for the Tris–Mes buffer at pH 8, the following relationship is obtained for conductivities ranging from 60 to 1000 $\mu S\,cm^{-1}$.

$$I\ (mol\,l^{-1}) = 2.10 \times 10^{-5} \chi\ (\mu S\,cm^{-1}) \tag{29}$$

This expression is supposed to be valid for buffered solutions which contain a solute. Indeed, addition of α-lactalbumin at 0.1 $g\,l^{-1}$ in Tris–Mes solution was found to have negligible influence on the electrical conductivity. However, addition of PLGA induces an increase of the electrical conductivity of about 20%. In that case, the initial ionic strength is calculated according to the initial electrical conductivity experimentally measured.

3.5. Filtration experiments

Filtration experiments are performed using a stirred cell (Amicon) with a membrane surface of 12.6 cm^2. Filtrations are carried out with the same membrane as that used during electroseparation experiments. The transmembrane pressure, set-up by air pressurisation, ranges from 0.05×10^5 to 0.2×10^5 Pa in order to have a solvent flux comparable to that obtained during electroseparation experiments. The influence of the ionic strength is studied by adding NaCl (0.1 M) to the buffer.

The solute transmission coefficients, for the pressure range used, are determined by measuring the feed (C_f) and permeate concentrations (C_p)

$$T = \frac{C_p}{C_f} \tag{30}$$

4. Results and discussion

An experimental work is carried out in order to investigate the different contributions to the solvent and solute mass transfer. The influence of the operating conditions, i.e. flow rate and voltage, as well as that of the solution composition are studied. Solutes of distinct size and/or electrical charge are used. Their relevant characteristics are reported in Table 1 for the conditions under study. The experimental variations of the outlet concentrations are plotted versus the characteristic parameter $E\tau$ pointed out from the theoretical approach (see Eq. (22)). These variations are compared to the calculated ones in order to determine the value of the partition coefficient.

4.1. Validation of the electrophoretic chamber design

It was former assumed that the only contribution to the convection, i.e. to the volume flow, is due to electro-osmosis. However, as far as a flow rate is established on both sides of a porous membrane, another kind of convection, due to the permeation resulting from any pressure difference between both sides of

Table 1
Characteristics of the solutes used for the experimental study molecular weight (M_W), isoelectric point (I_p) and electrophoretic mobility (u_{mi})[a]

Solute	M_W (Da)	I_p	u_{mi} at pH 8 ($m^2\,V^{-1}\,s^{-1}$)	u_{mi} at pH 4.8 ($m^2\,V^{-1}\,s^{-1}$)
PEG	1000	–	0	0
PLGA	1000	3.20	-5.6×10^{-8}	-4.7×10^{-8}
α-Lacta	14000	4.55	-1.85×10^{-8}	≈0

[a] PEG: polyethylenglycol; PLGA: poly(L-glutamic) acid; α-lacta: α-lactalbumin.

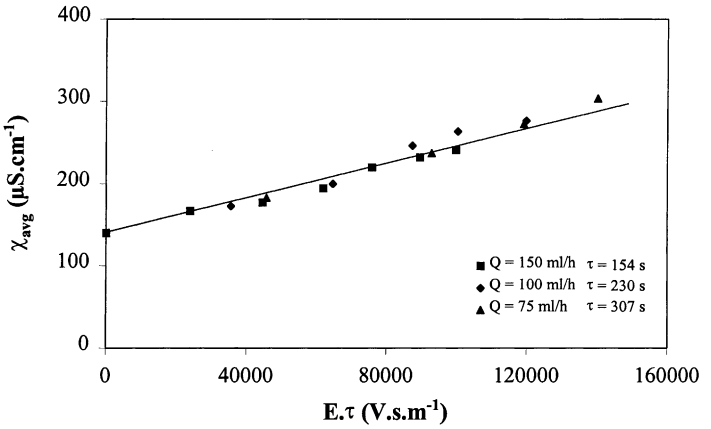

Fig. 3. Variation of the mean electrical conductivity vs. the product of the electric field by the residence time ($E\tau$). Operating condition: Tris–Mes at pH 8.

the permeable membrane, can also take place. This contribution was estimated in the conditions used, by measuring the inlet flow rates in both compartments without applying any current. It was found that the inlet flow rates are comparable to the outlet ones, the maximum difference remaining lower than 2%.

Another requirement concerns the proper control of the temperature increase and of the pH variation. It was demonstrated that for any set of operating conditions, these variations do not exceed 3°C and 0.1 pH unit, respectively.

Because of the arrangement of the ion exchange membranes, there is a migration of the buffer ions from the electrode compartments to the separation chamber. The resulting variation of the electrical conductivity is plotted in Fig. 3 versus the parameter $E\tau$. One can observe that a unique straight line is obtained whatever the operating conditions. It means that the electrophoretic mobility of the buffer ions remains constant over the experimental duration.

Finally, an example of experimental variations of the solute concentration versus time is plotted in Fig. 4,

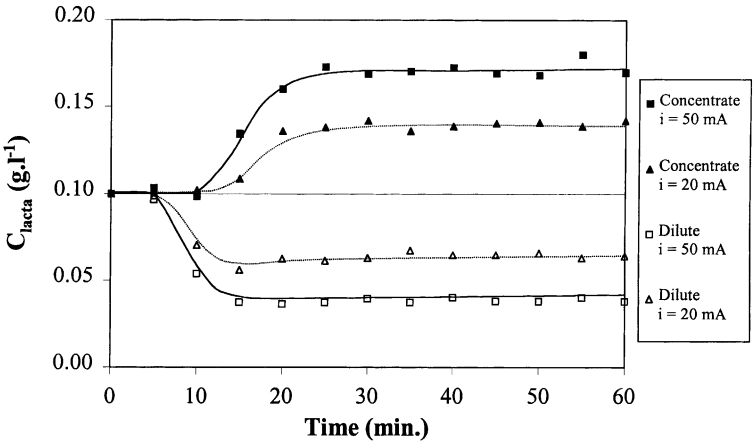

Fig. 4. Example of variation of the solute outlet concentration vs. time. Operating conditions: α-lactalbumin, $C_0 = 0.1\,\mathrm{g\,l^{-1}}$, Tris–Mes at pH 8, $Q = 100\,\mathrm{ml\,h^{-1}}$, $i = 20\,\mathrm{mA}$ ($E = 195\,\mathrm{V\,m^{-1}}$) and $i = 50\,\mathrm{mA}$ ($E = 305\,\mathrm{V\,m^{-1}}$).

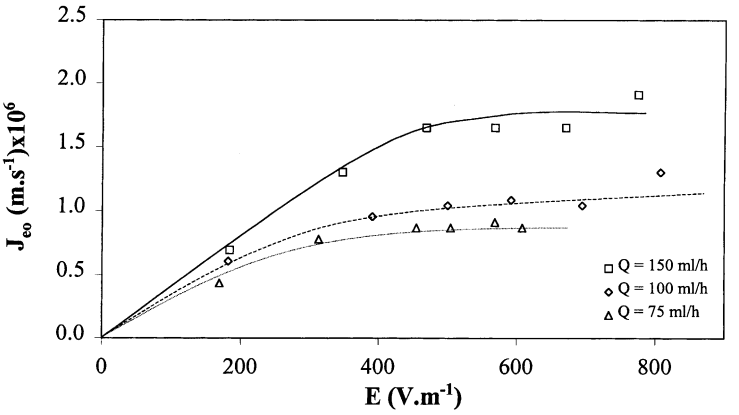

Fig. 5. Influence of the flow rate on the variations of the solvent flux vs. the electric field. Operating condition: Tris–Mes at pH 8.

showing that the concentrations in both compartments reach a constant value after about 20–30 min. Such a steady-state was observed for any set of conditions. Experimental values of the electro-osmotic flux and of the solute concentration presented hereafter are those obtained at steady-state.

4.2. Electro-osmotic flux

Figs. 5 and 6 show the experimental variations of the electro-osmotic flux versus the electric field for different values of the flow rate, obtained with the Tris–Mes buffer and with a buffered solution of PLGA, respectively. On the other hand, Fig. 7 gives the variations of the electro-osmotic flux versus the electric field obtained at a fixed flow rate with buffered solutions containing different solutes.

One can state that in any case, the electro-osmotic flux first increases with E before reaching a constant plateau value. This plateau value, that represents a limiting flux, increases for increasing flow rates. Fig. 7 also shows that the presence of PEG or α-lactalbumin has no measurable influence on the electro-osmotic flux. On the contrary, as far as PLGA is present in the buffer, significantly increased values of the electro-osmotic flux are obtained. Since the electro-osmotic flux measured with the buffer before and after any experiment remains constant, this

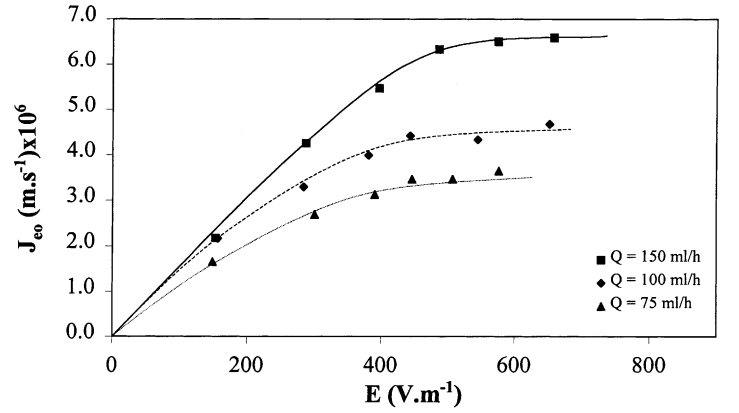

Fig. 6. Influence of the flow rate on the variations of the solvent flux vs. the electric field. Operating conditions: poly(L-glutamic) acid solution, $C_0 = 0.1\,g\,l^{-1}$, Tris–Mes at pH 8.

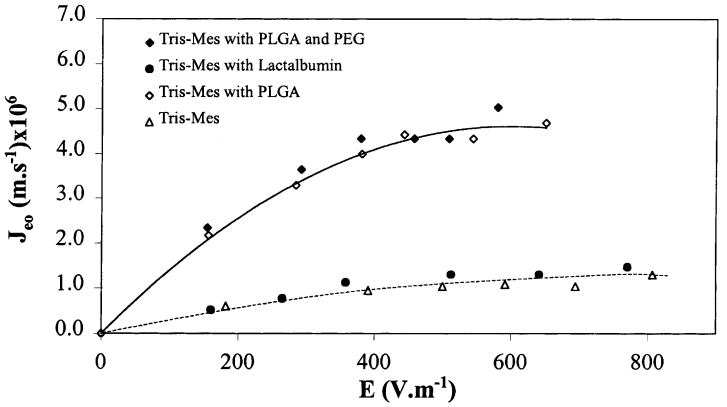

Fig. 7. Influence of the solute on the variation of the solvent flux vs. the electric field. Operating conditions: $C_0 = 0.1\,\mathrm{g\,l^{-1}}$, Tris–Mes at pH 8, $Q = 100\,\mathrm{ml\,h^{-1}}$.

variation does not come from an adsorption of the solute onto the membrane surface.

It was already demonstrated in previous studies that the membrane zeta potential can be increased when put into contact with a solution containing a charged solute [24,25]. Moreover, this increase was found to be dependent on the charge of the solute. Then, because of its direct relationship with the zeta potential (see Eq. (4)), such a dependence is expectable for the electro-osmotic flux. Present results indeed show a good qualitative correlation between the influence of the solute on J_{eo} and the solute charge, which can be estimated from its electrophoretic mobility. The highest variation is obtained with PLGA, which has the highest electrophoretic mobility for the conditions investigated (see Table 1). It seems that the charge of α-lactalbumin, whilst different from zero, is not sufficient to change the electro-osmotic flux, the value of which is identical to that obtained either with the buffer or with PEG, which is a neutral solute.

The other finding concerns the existence of a limiting flux. Such a limiting flux, the value of which depends on the feed flow rate, is quite known as far as pressure driven membrane operations are concerned [27–29]. The most common explanation is concentration polarisation, i.e. the coupling between convection and diffusion. It will be later demonstrated that the contribution of diffusion is quite negligible in the conditions of the present work.

Former studies were devoted to the variation of electro-osmotic flux or zeta potential versus operating parameters, like electric field or ionic strength for instance [30–33]. For a constant ionic strength, the electro-osmotic flux was found to be proportional to the electric field while for a fixed electric field value, decreasing electro-osmotic fluxes were obtained for increasing ionic strengths. On the other hand, it was previously explained that because of the arrangement of membranes used in the present study, the ionic strength increases over the experimental duration. Therefore, the relationship between the electro-osmotic mobility, calculated from experimental values of J_{eo} (Eq. (3)), and the ionic strength, estimated by Eq. (29) from the experimental measurement of the average conductivity, was investigated. Fig. 8 gives an example of the variations of the electro-osmotic mobility and of the ionic strength versus the parameter $E\tau$. Identical variations are obtained with any other fluid composition, i.e. a linear dependence of both parameters versus $E\tau$ represented by a unique straight line whatever the operating conditions. Thus, a direct relationship is pointed out between the ionic strength and the electro-osmotic mobility. Such results showing that the electro-osmotic mobility decreases for increasing ionic strength are in good agreement with previous ones [30] obtained in the same range of ionic strength, i.e. between 3×10^{-3} and $10^{-2}\,\mathrm{mol\,l^{-1}}$.

Then, the variation of the electro-osmotic mobility versus $E\tau$ can be represented by an equation of the

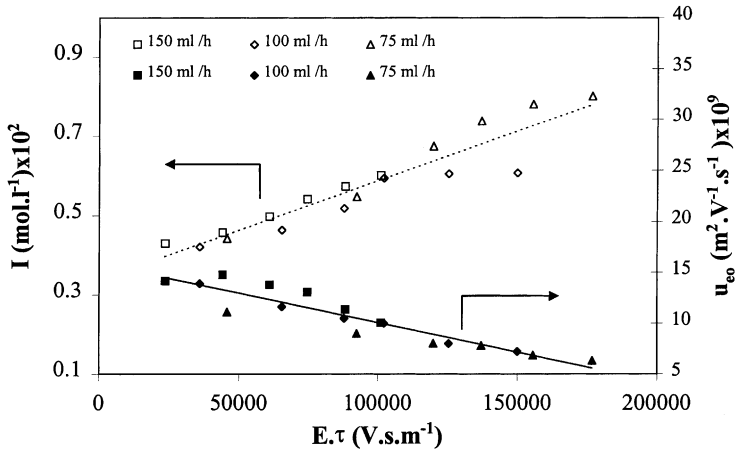

Fig. 8. Variation of the ionic strength (I) (empty symbols) and of the electro-osmotic mobility (u_{eo}) (full symbols) vs. the product of the electric field by the residence time ($E\tau$). Operating conditions: α-lactalbumin solution; $C_0 = 0.1\,g\,l^{-1}$; Tris–Mes at pH 8.

Table 2
Values of α and α_0 in Eq. (31)

Solution	α ($m^2\,V^{-1}\,s^{-1}$)	α_0 ($m^2\,V^{-1}\,s^{-1}$)
Tris–Mes	1.44×10^{-14}	0.40×10^{-8}
Tris–Mes with PLGA	5.80×10^{-14}	1.58×10^{-8}
Tris–Mes with α-lacta	1.37×10^{-14}	0.42×10^{-8}

following form:

$$u_{eo} = -\alpha E\tau + \alpha_0 \tag{31}$$

where α_0 represents the electro-osmotic mobility corresponding to the inlet ionic strength, i.e. that of the feed solution. This relationship is established for $E\tau$ values lower than $2 \times 10^5\,V\,s\,m^{-1}$.

Combined with Eq. (3), one gets for the electro-osmotic flux

$$J_{eo} = u_{eo}E = -\alpha E^2\tau + \alpha_0 E \tag{32}$$

Then, the limiting flux, J_{eo}^{lim}, as well as the corresponding electric field, E_{lim}, are obtained

$$E_{lim} = \frac{\alpha_0}{2\alpha\tau} \quad \text{and} \quad J_{eo}^{lim} = \frac{\alpha_0^2}{4\alpha\tau} \tag{33}$$

The values of α and α_0 determined from the experimental variations of u_{eo} versus $E\tau$ like those plotted in Fig. 8 for instance, are reported in Table 2 for the different solutions investigated. On the other hand, Table 3 gives the values of J_{eo}^{lim} and E_{lim} calculated by Eq. (33) for the different flow rates investigated. Comparison between experimental and calculated variations of the electro-osmotic flux versus E shows that the maximum difference does not exceed 20%. An example of comparison is provided in Fig. 9.

4.3. Solute mass transfer

The expression of the solute concentration, established in Section 2, is reminded hereafter

Table 3
Values of J_{eo}^{lim} and E_{eo}^{lim} calculated by Eq. (33)

Solution	J_{eo}^{lim} ($m\,s^{-1}$) $\times 10^6$			E_{lim} ($V\,m^{-1}$)		
	$\tau = 307\,s$	$\tau = 230\,s$	$\tau = 154\,s$	$\tau = 307\,s$	$\tau = 230\,s$	$\tau = 154\,s$
Tris–Mes	0.9	1.2	1.8	452	604	902
Tris–Mes with PLGA	3.5	4.7	7.0	444	592	884
Tris–Mes with α-lacta	1.0	1.4	2.1	500	666	995

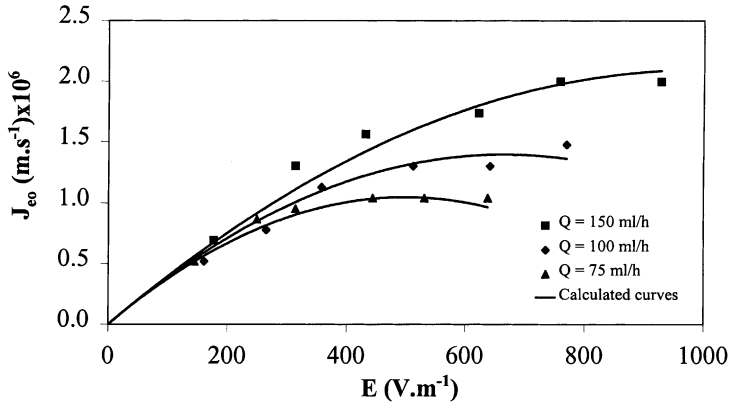

Fig. 9. Influence of the flow rate on the variations of the solvent flux vs. the electric field. Comparison between experimental and calculated values. Operating conditions: α-lactalbumin solution; $C_0 = 0.1\,\mathrm{g\,l^{-1}}$; Tris–Mes at pH 8.

$$C_d = C_0 \left[1 - \frac{u_{eo} E \tau}{d} \right]^{[(\phi(u_{mi}/u_{eo})-1)+1]}$$

It was considered that the solute transfer results from the coupling of electro-osmosis and electromigration of the charged solute. It means that the contribution of osmosis and diffusion to the solution and solute transfer were neglected with respect to those of electro-osmosis and electromigration. In order to check this assumption, a dedicated experiment was carried out (see Section 3.3). It was observed that the flow rates as well as the concentrations remain constant in both compartments.

From the experimental study concerning the electro-osmotic flux, the following relationship was also established:

$$u_{eo} = -\alpha E \tau + \alpha_0$$

Figs. 10 and 11 show the variations of the outlet concentrations versus the parameter $E\tau$ for the two charged solutes investigated. For every experiment, the solute mass balance was checked within 10%. Results obtained with PEG are not presented since the outlet concentration was found to remain constant and equal to the inlet one. One can observe that for a given solute,

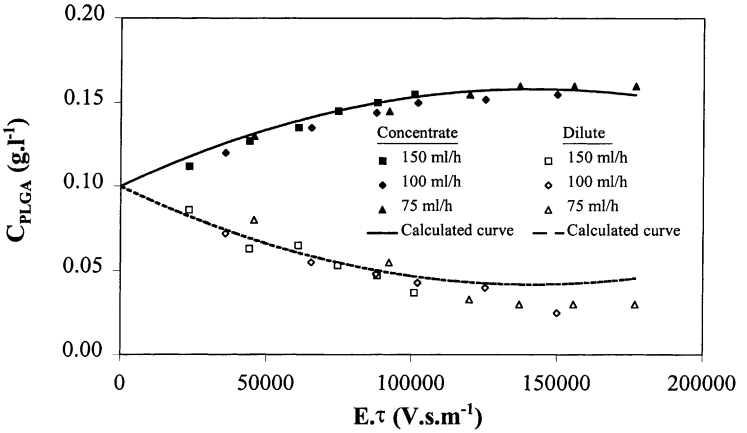

Fig. 10. Comparison between experimental (points) and calculated (curves) variations of the outlet concentrations vs. the product of the electric field by the residence time ($E\tau$). Operating conditions: poly(L-glutamic) acid solution; $C_0 = 0.1\,\mathrm{g\,l^{-1}}$; Tris–Mes at pH 8.

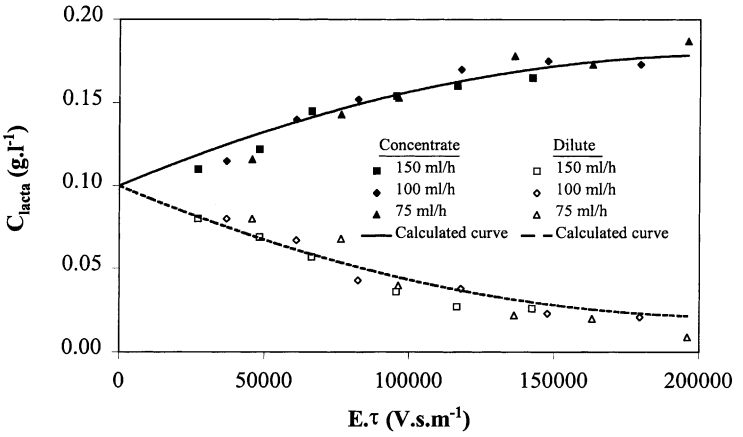

Fig. 11. Comparison between experimental (points) and calculated (curves) variations of the outlet concentrations vs. the product of the electric field by the residence time ($E\tau$). Operating conditions: α-lactalbumin solution; $C_0 = 0.1\,\mathrm{g\,l^{-1}}$; Tris–Mes at pH 8.

the experimental values obtained for different electric fields and flow rates are located on a single curve. Then, the general expression established for the concentration (Eq. (22) is validated with a unique value of the partition coefficient. In general, this coefficient, the value of which is comprised between 0 and 1, just provides a quantitative evaluation of the strength of the interactions taking place at the membrane–solution interface. However, as far as its dependence with respect to some relevant physicochemical parameters is investigated, this partition coefficient can be quite helpful to identify the physical origin of the phenomena governing the mass transfer. It is thus, calculated for each solute from the above experimental results by fitting the experimental variations of the concentration with those calculated by Eq. (22). The corresponding value of u_{eo} is given by Eq. (31) (see Table 2 for α and α_0). The electrophoretic mobility is that reported in Table 1. Indeed, in the range of ionic strength investigated, this mobility may be considered as constant. The partition coefficients deduced from experimental results are reported in Table 4. The corresponding calculated variations of the concentration are plotted in Figs. 10 and 11. One can state that in spite of their close molecular weights, quite distinct partition coefficients are obtained for PEG and PLGA, i.e. 1 and 0.02, respectively. Then, the low and even almost nil transfer of PLGA through the membrane does not come from steric effects. This is confirmed by the results obtained with α-lactalbumin, the molecular weight of which is about 14 times that of PLGA. Indeed, with this later solute the partition coefficient is much higher than that of PLGA and more comparable to that obtained with PEG. Then, the hindered transfer of PLGA comes from an electrostatic repulsion by the negatively charged UF membrane.

For sake of validation, filtration experiments (see Section 3) are carried out using the same UF membrane and solutes than those used during electromigration experiments. Since charge effects are investigated, buffered solutions with different pH and ionic strengths are used. The experimental values of the

Table 4
Fitted partition coefficients ϕ and mean transmission coefficients T influence of the buffer and solute characteristics

Solute	ϕ (pH = 8)	T (pH = 8)	T (pH = 4.8)	T (pH = $8_{\mathrm{NaCl\,(0.1\,M)}}$)
PEG	1	1	1	1
PLGA	0.02	0.2	0.3	0.5
α-Lacta	0.8	0.4	0.7	0.8

transmission coefficients are reported in Table 4 for the different solutes and buffer conditions. Whilst distinct values are obtained, a good qualitative correlation is observed between the values of the partition coefficient and those of the transmission coefficient at pH 8. The difference comes from the distinct driving forces and hydrodynamic conditions involved in both operations.

The predominance of charge effects is clearly pointed out. For the neutral solute, PEG, the transmission remains constant and equal to 1. On the opposite, for the charged solutes, i.e. PLGA and α-lactalbumin, any variation of the pH or the ionic strength results in a modification of the transmission coefficient. Decreasing the pH from 8 to 4.8 results in decreasing the solute charge. Then, the electrostatic repulsion is lowered and higher transmission coefficients are obtained. This increase of the solute transfer is more pronounced with α-lactalbumin than with PLGA because of the strongest variation of the former solute charge between the two pH values (see Table 1). The same tendency is pointed out from the influence of the ionic strength. Indeed, as far as the ionic strength increases, the solute charge decreases. Then, electrostatic interactions are lowered so that increasing values of the transmission coefficient are obtained.

Figs. 10 and 11 also show that almost identical variations are obtained for the outlet concentrations of α-lactalbumin and PLGA. However, these variations result from quite distinct limiting transfer phenomena. Indeed, concerning α-lactalbumin, it was demonstrated that the variation of the concentration is mainly due to the solute flux due to the electrophoretic migration through the membrane, since the partition coefficient is close to 1 and the electro-osmotic solvent flux is low. On the opposite, for PLGA, the solute transfer through the membrane was found to be negligible so that the concentration variation results almost exclusively from the electro-osmotic solvent flux, which is much higher than that obtained with α-lactalbumin.

5. Conclusion

The aim of this work was to study the mass transfer mechanisms involved in electrophoretic separations using a porous filtration membrane as a contactor.

On one hand, a theoretical approach was carried out. The different contributions to the mass transfer were first identified and discussed. A model was then developed in which the solute transport is considered to result from the coupling of the convection due to electro-osmosis with the electrophoretic migration. In this manner, an expression was established that gives the solute concentration as function of the following parameters: $E\tau$, which is the product of the electric field by the residence time, the electrophoretic mobility of the solute, the electro-osmotic mobility and a partition coefficient, these later two depending on both the membrane and the buffer and solute characteristics.

On the other hand, an experimental work was performed using a dedicated prototype electroseparation apparatus and different solutes, chosen with respect to their size and electrical charge. It was observed that for a given solute, the influence of the operating conditions can be properly represented through the only parameter $E\tau$, which was already pointed out as characteristic of electrophoretic separations. The experimental results concerning the variation of the electro-osmotic flux versus the electric field showed the existence of a limiting flux. It was demonstrated that this limiting value comes from the variation of the ionic strength resulting from the migration of buffer ions from the electrode compartments. An expression was established to calculate the variation of the electro-osmotic mobility versus the parameter $E\tau$. The results obtained with the different solutes pointed out the influence of the solute charge on the electro-osmotic flux. Indeed, increasing fluxes were obtained with solutes of increasing electrophoretic mobility. The partition coefficient was then determined for each solute by fitting the experimental variations of the concentration with the ones calculated by the model. These values were compared with those of the transmission coefficient obtained during filtration experiments. The influence of the pH and ionic strength, which fixes the solute charge, was investigated. It was thus, concluded that the solute transfer is governed by electrostatic interactions taking place at the membrane–solution interface.

Finally, for the conditions used in this work, it was found that whilst resulting from quite distinct phenomena, almost identical concentration variations can be obtained even with solutes having significant different charge and size.

Then, further work is still necessary before considering the fractionation of fluids of practical interest. This work will be devoted to the improvement of

the process performances with such solutions as those used in the present study for which the limitations as well as their dependence with respect to the main parameters of the system were clearly identified.

References

[1] O. Vesterberg, A short history of electrophoretic methods, Electrophoresis 14 (1993) 1243.

[2] K. Hannig, Preparative electrophoresis, in: M. Bier (Ed.), Electrophoresis: Theory, Methods and Applications, Vol. II, Academic Press, New York, 1967, p. 423.

[3] R. Horuk, Preparative gel electrophoresis, in: A. Chrambach, M.J. Dunn, B.J. Radola (Eds.), Advances in Electrophoresis, Vol. 1, VCH, Weinheim, 1987, p. 361.

[4] P.G. Righetti, M. Faupel, E. Wenisch, Preparative electrophoresis, in: A. Chrambach, M.J. Dunn, B.J. Radola (Eds.), Advances in Electrophoresis, Vol. 5, VCH, Weinheim, 1992, p. 159.

[5] M.J. Clifton, N. Jouve, H. de Balmann, V. Sanchez, Conditions for purification of proteins by free flow zone electrophoresis, Electrophoresis 11 (1990) 913.

[6] H. Roux-de Balmann, V. Sanchez, Continuous-flow electrophoresis: a separation criterion applied to the separation of model proteins, J. Chromatogr. 594 (1992) 351.

[7] S. Nath, H. Schütte, H. Hustedt, W.D. Deckwer, Application of continuous zone electrophoresis to preparative separation of proteins, Biotechnol. Bioeng. 42 (1993) 829.

[8] F. Dalens, H. Roux-de Balmann, V. Sanchez, Improved operating conditions for preparative separation of proteins by continuous flow zone electrophoresis, Biosep. 5 (1995) 127.

[9] H. Roux-de Balmann, R.M. Cerro, V. Sanchez, Purification of bioproducts by free flow zone electrophoresis: choice of processing parameters, Electrophoresis 19 (1998) 1117.

[10] N. Jouve, M.J. Clifton, Three-dimensional modelling of coupled flow field and heat transfer in continuous-flow electrophoresis, J. Int. Heat Mass Transfer 34 (1991) 2461.

[11] M.J. Clifton, N. Jouve, V. Sanchez, Influence of buoyancy-driven convection on protein separation by free flow electrophoresis, Adv. Space Res. 12 (1) (1992) 373.

[12] C.F. Ivory, The prospects for large-scale electrophoresis, Sep. Sci. Technol. 23 (1988) 875.

[13] Z.S. Horvath, G.L. Corthals, C.W. Wrigley, J. Margolis, Multifunctional apparatus for electrokinetic processing of proteins, Electrophoresis 15 (1994) 968.

[14] Z. Liu, Z. Huang, J. Chong, H. Yang, F. Ding, N. Yuan, Continuous separation of proteins by multichannel flow electrophoresis, Sep. Sci. Technol. 31 (1996) 1427.

[15] Y.H. Yen, M. Cheryan, Separation of lactic acid from whey permeate fermentation broth by electrodialysis, Trans. IChemE 69 (1991) 200.

[16] C.A.P.M. van Nunen, Design of a large-scale membrane-electrophoresis module for separation of proteins, Thesis, Eindhoven School for Technological Design, The Netherlands, 1997.

[17] R.J. Hunter, Zeta potential in Colloid Science: Principle and Applications, Academic Press, London, 1981.

[18] W.R. Bowen, R.A. Clark, Electro-osmosis at microporous membranes and the determination of zeta potential, J. Colloid Int. Sci. 97 (1984) 401.

[19] K.J. Kim, A.G. Fane, M. Nyström, A. Pihlajamaki, W.R. Bowen, H. Mukhtar, Evaluation of electro-osmosis and streaming potential for measurement of electric charges of polymeric membranes, J. Membr. Sci. 116 (1996) 149.

[20] A.J. O'Connor, H.R.C. Pratt, G.W. Stevens, Electrophoretic mobilities of proteins and protein mixtures in porous membranes, Chem. Eng. Sci. 51 (1996) 3459.

[21] J.D. Ferry, Ultra-filter membranes and ultra-filtration, Chem. Rev. 18 (1936) 373.

[22] W.D. Munch, L.P. Zestar, J.L. Anderson, Rejection of polyelectrolytes from microporous membranes, J. Membr. Sci. 5 (1979) 77.

[23] F.G. Smith, W.M. Deen, Electrostatic effects on the partitioning of spherical colloids between dilute bulk solution and cylindrical, J. Colloid Interface Sci. 91 (1983) 571.

[24] C. Causserand, M. Nyström, P. Aimar, Study of streaming potential of clean and fouled ultra-filtration membranes, J. Membr. Sci. 88 (1994) 211.

[25] K.J. Kim, A.G. Fane, M. Nyström, A. Pihlajamaki, Chemical and electrical characterisation of virgin and protein-fouled polycarbonate track-etched membranes by FT-IR and streaming potential measurements, J. Membr. Sci. 134 (1997) 199.

[26] V.S. Stoll, J.S. Blanchard, Buffers: principle and practice, Methods Enzymol. 182 (1990) 24.

[27] J.G. Wijmans, S. Nakao, G.B. van den Berg, F.R. Troelstra, C.A. Smolders, Hydrodynamic resistance of concentration polarisation layers in ultra-filtration, J. Membr. Sci. 22 (1985) 117.

[28] P. Aimar, J.A. Howell, Concentration polarisation build-up in hollow fibres: a method of measurement and its modelling in ultra-filtration, J. Membr. Sci. 59 (1991) 81.

[29] H. de Balmann, V. Sanchez, Coupling between concentration polarisation and blockage in ultra-filtration, Int. Chem. Eng. 32 (1992) 665.

[30] M. Tasaka, S. Tamura, N. Takemura, K. Morimoto, Concentration dependence of electro-osmosis and streaming potential across charged membranes, J. Membr. Sci. 12 (1982) 169.

[31] M. Nyström, M. Linström, E. Matthiasson, Streaming potential as a tool in the characterisation of ultra-filtration membrane, Colloids Surf. 36 (1989) 297.

[32] M. Pontie, L. Durand-Bourlier, D. Lemordant, J.M. Laine, Phénomènes électrocinétiques dans les membranes organiques composites microporeuses à faible densité de charge, J. Chim. Phys. 94 (1997) 1741.

[33] A. Szymczyk, P. Fievet, M. Mullet, J.C. Reggiani, J. Pagetti, Comparison of two electrokinetic methods, electro-osmosis and streaming potential, to determine the zeta potential of plane ceramic membranes, J. Membr. Sci. 143 (1998) 189.